Broadband down-conversion for silicon solar cell by ZnSe/phosphor heterostructure

Xiaojie Wu,[1] Fanzhi Meng,[1] Zhenzhong Zhang,[2,*] Yingning Yu,[1] Xiaojuan Liu,[1] and Jian Meng[1,3]

[1]*State Key Laboratory of Rare Earth Resources Utilization, Changchun Institute of Applied Chemistry, Chinese Academy of Sciences, 5625 Renmin Street, Changchun 130022, China*

[2]*State Key Laboratory of Luminescence and Applications, Changchun Institute of Optics, Fine Mechanics and Physics, Chinese Academy of Sciences, 3888 Dongnanhu Road, Changchun 130033, China*

[3]*jmeng@ciac.jl.cn*

[*]*zhangzz@ciomp.ac.cn*

Abstract: Down-conversion is a feasible way to improve conversion efficiency of silicon solar cell. However, the width of excitation band for down-converter based on trivalent lanthanide ions is still not satisfying. Here, we designed and fabricated a heterostructural down-converter composed of Y_2O_3: [(Tb^{3+}-Yb^{3+}), Li^+] quantum cutting phosphor and ZnSe. The ZnSe phase was used to absorb the incident light with energy larger than its bandgap, and transfer the energy to Tb^{3+}-Yb^{3+} quantum cutting couple. Short-wavelength incident light was finally converted into a strong Yb^{3+} emission at about 1000 nm, locating at the maximal spectral response of silicon solar cell. The excitation band of the down-conversion covers a wide region of 250-550 nm. Benefiting from the energy match between ZnSe bandgap and $^7F_6 \rightarrow {}^5D_4$ absorption of Tb^{3+} ions, the bandwidth of down-conversion is almost maximized.

OCIS codes: (160.2540) Fluorescent and luminescent materials; (160.5690) Rare-earth-doped materials; (160.6000) Semiconductor materials; (350.6050) Solar energy

References and links

1. R. T. Wegh, H. Donker, K. D. Oskam, and A. Meijerink, "Visible quantum cutting in LiGdF4:Eu^{3+} through downconversion," Science **283**(5402), 663–666 (1999).
2. C. Strümpel, M. McCann, G. Beaucarne, V. Arkhipov, A. Slaoui, V. Švrček, C. Del Canizo, and I. Tobiasd, "Modifying the solar spectrum to enhance silicon solar cell efficiency-An overview of available materials," Sol. Energy Mater. Sol. Cells **91**(4), 238–249 (2007).
3. B. M. van der Ende, L. Aarts, and A. Meijerink, "Lanthanide ions as spectral converters for solar cells," Phys. Chem. Chem. Phys. **11**(47), 11081–11095 (2009).
4. T. Trupke, M. A. Green, and P. Würfel, "Improving solar cell efficiencies by down-conversion of high-energy photons," J. Appl. Phys. **92**(3), 1668 (2002).
5. B. Fan, C. Chlique, O. Merdrignac-Conanec, X. Zhang, and X. Fan, "Near-infrared quantum cutting material Er^{3+}/Yb^{3+} doped La_2O_2S with an external quantum yield higher than 100%," J. Phys. Chem. C **116**(21), 11652–11657 (2012).
6. X. Y. Huang, S. Y. Han, W. Huang, and X. G. Liu, "Enhancing solar cell efficiency: the search for luminescent materials as spectral converters," Chem. Soc. Rev. **42**(1), 173–201 (2012).
7. B. M. van der Ende, L. Aarts, and A. Meijerink, "Near-infrared quantum cutting for photovoltaics," Adv. Mater. **21**(30), 3073–3077 (2009).
8. P. Vergeer, T. J. H. Vlugt, M. H. F. Kox, M. I. Den Hertog, J. P. J. M. Vander Eerden, and A. Meijerink, "Quantum cutting by cooperative energy transfer in $Yb_xY_{1-x}PO_4$:Tb^{3+}," Phys. Rev. B **71**(1), 014119 (2005).
9. D. L. Dexter, "Possibility of luminescent quantum yields greater than unity," Phys. Rev. **108**(3), 630–633 (1957).
10. Q. H. Zhang, J. Wang, G. G. Zhang, and Q. Su, "UV photon harvesting and enhanced near-infrared emission in novel quantum cutting Ca_2BO_3Cl:Ce^{3+}, Tb^{3+}, Yb^{3+} phosphor," J. Mater. Chem. **19**(38), 7088 (2009).
11. Y. Chen, J. Wang, C. M. Liu, J. K. Tang, X. J. Kuang, M. M. Wu, and Q. Su, "UV-Vis-NIR luminescence properties and energy transfer mechanism of $LiSrPO_4$:Eu^{2+}, Pr^{3+} suitable for solar spectral convertor," Opt. Express **21**(3), 3161–3169 (2013).
12. Z. H. Bai, M. Fujii, T. Hasegawa, K. Imakita, M. Mizuhata, and S. Hayashi, "Efficient ultraviolet-blue to near-infrared downconversion in Bi–Dy–Yb-doped zeolites," J. Phys. D Appl. Phys. **44**(45), 455301 (2011).
13. R. Martín-Rodríguez, R. Geitenbeek, and A. Meijerink, "Incorporation and luminescence of Yb^{3+} in CdSe nanocrystals," J. Am. Chem. Soc. **135**(37), 13668–13671 (2013).

#201619 - $15.00 USD Received 19 Nov 2013; revised 11 Feb 2014; accepted 20 Feb 2014; published 1 Apr 2014

14. Q. Luo, X. S. Qiao, X. P. Fan, and X. H. Zhang, "Near-infrared emission of Yb^{3+} through energy transfer from ZnO to Yb^{3+} in glass ceramic containing ZnO nanocrystals," Opt. Lett. **36**(15), 2767–2769 (2011).
15. F. Xiao, R. Chen, Y. Q. Shen, Z. L. Dong, H. H. Wang, Q. Y. Zhang, and H. D. Sun, "Efficient energy transfer and enhanced infrared emission in Er-doped ZnO-SiO_2 composites," J. Phys. Chem. C **116**(24), 13458–13462 (2012).

1. Introduction

Photovoltaic devices have attracted considerable interest in recent years because of their potential to harvest energy from sunlight, a clean and sustainable power source. Among the members of the photovoltaic device family, silicon solar cell is the most common one. A mismatch between the incident solar spectrum and silicon spectral response is considered the main reason for the low conversion efficiency. Silicon absorbs photons with higher energy than its bandgap (i.e. 1.17eV) and converts each absorbed photon to a pair of carriers. Thus, photons with energy lower than the bandgap are not absorbed, while photons with energy higher than 1.17 eV loss their excess energy through thermalization of hot carriers. To increase the efficiency of single-junction solar cells, the incident solar spectrum should be modified to match the spectral response of the device. Extensive efforts have been devoted to the study of upconversion where low energy photons are combined to produce photons with energy above the bandgap, and for down-conversion where use is made of the excess energy to excite additional carriers [1–9]. Compared with up-conversion, down-conversion of solar spectrum is more promising because it does not require high power density for solar radiation and thus avoids the use of solar light concentrators. Conversion efficiency in quantum cutting (QC) down-conversion could even approach 200%.[9] QC down-conversion based on Ln^{3+}-Yb^{3+} (Ln = Tb, Tm, Pr, Er, Ho, and Nd) couple systems is able to split one incident high-energy photon into two or more near-infrared (NIR) photons [5–8]. The Yb^{3+} emission, locating in the region of 900 nm to 1100 nm, matches the maximal spectral response of silicon devices well. However, the forbidden f–f transitions of the trivalent lanthanide ions limit the width of the absorption band of the phosphors. Several rare earth ions with 4f–5d transition (such as Ce^{3+}, Eu^{2+}, and Bi^{3+}) have been used as sensitizers with broadband absorption [10–12]. In fact, a semiconductor can act as a good sensitizer for the above converters. The large density of state in conduction and valance bands ensure a sufficiently high light absorption. CdSe and ZnO have been used to broaden the absorption band for rare earth phosphors [13–15]. However, due to the mismatch between the semiconductor bandgap and absorption of rare earth ions, the excitation bandwidth of the converters is still not satisfying.

In this presentation, ZnSe, a direct bandgap semiconductor with a bandgap of 2.6~2.7 eV, was used as the sunlight absorber and energy donor for Tb^{3+}-Yb^{3+} QC phosphor. Considering that the solid solubility of rare earth ions is small in group II-VI semiconductors, the down converter was fabricated into ZnSe/phosphor heterostructure by hot pressing method. Owing to the good energy match between the ZnSe bandgap and Tb^{3+} $^7F_6$–$^5D_4$ absorption (~2.58 eV), the excitation band for Yb^{3+} $^2F_{2/5}\rightarrow{}^2F_{7/2}$ emission covers a broad region of 250-550 nm. In practical applications, a light down-converter should be a transparent material, bonding on the surface of solar cell. Therefore, we further fabricated the ZnSe/phosphor converter into a double-layer thin film. Similar broadband excitation effect was obtained.

2. Experiments

The ZnSe/Y_2O_3:[(Tb^{3+}-Yb^{3+}), Li^+] heterostructures were synthesized by hot pressing on a spark plasma sintering furnace (SPS). As one of the two precursors, the Y_2O_3:[(Tb^{3+}-Yb^{3+}), Li^+] phosphor powder was prepared by sol-gel method. 2mol% Li^+ was used to improve the emission performance of Yb^{3+}.[15] The obtained phosphor powder was pre-annealed in oxygen atmosphere at 500 °C and then annealed at 1000 °C for 10 hours, followed by a vacuum annealing at 1000 °C for 1.5 hours. ZnSe powder with 99.999% purity was used as the other precursor. The two precursors were mixed in a mole ratio of 85:15 and finely milled together in argon atmosphere, and then were compacted under a unidirectional pressure of 150 MPa at

#201619 - $15.00 USD Received 19 Nov 2013; revised 11 Feb 2014; accepted 20 Feb 2014; published 1 Apr 2014

850 °C for 15 minutes. According to the content of Tb and Yb in the phosphor phase, the final samples were labeled by A(Tb:0.01, Yb:0.00), B(Tb:0.01, Yb:0.04), C(Tb:0.01, Yb:0.06), D (Tb:0.01, Yb:0.10) and E(Tb:0.005, Yb:0.06), in sequence.

The ZnSe/Y_2O_3:[(Tb^{3+}-Yb^{3+}), Li^+] double layer film was composed of Y_2O_3:[(Tb^{3+}-Yb^{3+}), Li^+] phosphor film on sapphire substrate and a ZnSe cap layer. The Y_2O_3:[(Tb^{3+}-Yb^{3+}), Li^+] film was grown by magnetron sputtering method, where Metallic terbium, ytterbium and yttrium (99.99%) were used as the targets. The ZnSe cap layer was grown by physical vapor deposition, where ZnSe powder with 99.999% purity was used as the precursor.

The X-ray diffraction (XRD) was performed on a Bruker D8 Focus diffractometer using Cu Kα radiation (0.15405 nm). The morphology was studied by using a Hitachi S-4800 scanning electron microscope. The photoluminescence (PL) and PL excitation spectra were measured on an FLSP 920 spectrometer. The PL decay curves were recorded by a Lecroy Wave Runner 6100 digital oscilloscope (1 GHz). A tunable laser (Continuum Sunlite OPO) with pulse width of 4 ns was used as the excitation source.

3. Results and discussion

The down-conversion process was designed as shown in Fig. 1. Short-wavelength incident light should be adequately utilized to increase the conversion efficiency. Benefiting from the large density of states in semiconductor, photons with energy higher than ZnSe bandgap (i.e. λ<470 nm) can be fully absorbed. The absorbed solar energy is transferred to the Tb^{3+}-Yb^{3+} QC phosphor through recombination of photogenerated carriers and is cut into Yb^{3+} NIR emission. The above processes are depicted by the chart in the middle. The NIR emission approaches the maximal spectral response (~1000 nm) of the silicon device. Photons with energy lower than ZnSe bandgap pass through the down-converter because of high transparency of ZnSe in this waveband. These photons can be directly absorbed by the silicon solar cell. The QC down-conversion bandwidth is almost maximized because the ZnSe bandgap matches well $^7F_6 \rightarrow {}^5D_4$ absorption of Tb^{3+} ions.

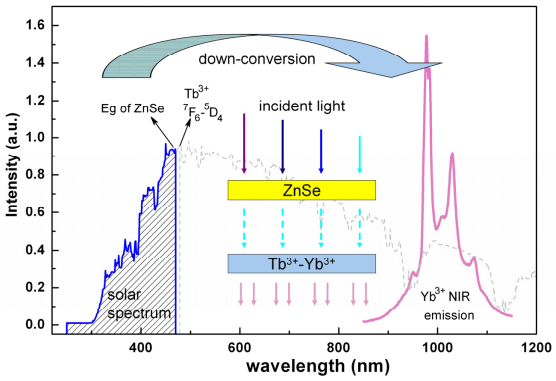

Fig. 1. Sketch of the down-conversion process design. Due to the energy match between ZnSe bandgap and $^7F_6 \rightarrow {}^5D_4$ absorption of Tb^{3+} ions, the bandwidth of down-conversion is almost maximized.

Figure 2 shows a typical XRD pattern of the heterostructural down-converter, recorded on sample C. As indexed, the diffraction peaks agree well with ZnSe and Y_2O_3. No diffraction peak from any other phase was observed. This result indicates that the down-converter is composed of only ZnSe and Y_2O_3:[(Tb^{3+}-Yb^{3+}), Li^+] phases. The inset in Fig. 2 shows a typical top-view SEM image of the samples. The large grains with sizes of 3-5 μm are of ZnSe, and the small grains with sizes of 100-200 nm are of Y_2O_3:[(Tb^{3+}-Yb^{3+}), Li^+] phosphor.

#201619 - $15.00 USD Received 19 Nov 2013; revised 11 Feb 2014; accepted 20 Feb 2014; published 1 Apr 2014

The ZnSe grains are tightly sintered with one another, and the phosphor grains are embedded in the ZnSe grains, such as in the plum pudding model.

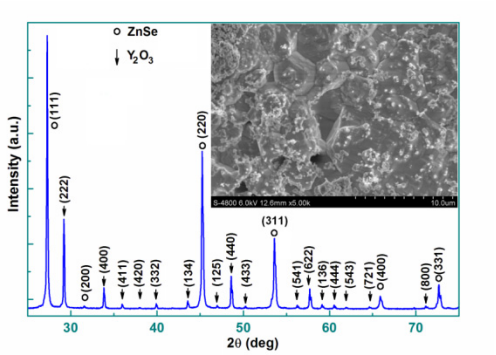

Fig. 2. Theta-2theta XRD pattern indicates that the heterostructural down-converter is composed of only ZnSe and Y_2O_3:[(Tb^{3+}-Yb^{3+}), Li^+] phases . Inset: typical top-view SEM image of sample C, showing a plum-pudding-like morphology.

PL spectra, excitation spectra, and PL decay were recorded to verify the designed energy transfer (ET) process in these ZnSe/phosphor heterostructure samples.

Figure 3(a) shows the PL and excitation spectra of Yb^{3+} NIR emission obtained on sample C. Under excitation at 280 and 460 nm, strong NIR emission from Yb^{3+} $^2F_{5/2}\rightarrow{}^2F_{7/2}$ transition was observed [right side of Fig. 3(a)]. The excitation spectrum was obtained by monitoring the 977 nm emission. A broad excitation band ranging from 250 nm to 550 nm is observed. Note the spectrum intensity under visible excitation is comparable with that under UV excitation.

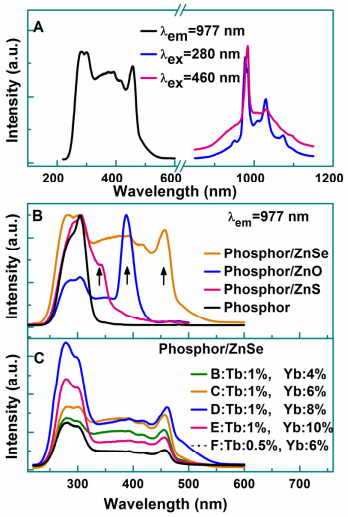

Fig. 3. (A) PL and Excitation spectra of Yb^{3+} $^2F_{5/2}\rightarrow{}^2F_{7/2}$ emission in sample C. (B) Excitation spectra of Yb^{3+} NIR emission in the single Y_2O_3:[(Tb^{3+}-Yb^{3+}), Li^+] phosphor (Tb:0.01, Yb:0.06) and the semiconductor(ZnS, ZnO, ZnSe)/phosphor(Tb:0.01, Yb:0.06) heterrostructures. (C) Excitation spectra of the ZnSe/phosphor heterostructures with different Tb and Yb fraction.

Semiconductors with different bandgaps were combined with the Y_2O_3:[(Tb^{3+}-Yb^{3+}), Li^+] phosphor through the same process to investigate whether the broadening of the excitation band for Yb^{3+} 977-nm emission is caused by combination with ZnSe. Figure 3(b) shows the

#201619 - $15.00 USD Received 19 Nov 2013; revised 11 Feb 2014; accepted 20 Feb 2014; published 1 Apr 2014

excitation spectra of Yb^{3+} $^2F_{5/2}\rightarrow{}^2F_{7/2}$ emission in a single phosphor (Tb:0.01, Yb:0.06) and the semiconductor (ZnS, ZnO, ZnSe)/phosphor (Tb:0.01, Yb:0.06) heterostructures. For the single phosphor without combining with semiconductor, the excitation spectrum is dominated by the UV peak. The emission intensity decreases abruptly when the excitation wavelength exceeds 310 nm. By contrast, the excitation band of the semiconductor/phosphor heterostructures shows different broadening. Aside from the excitation peak at 306 nm, another peak can be observed at 343, 388, and 460 nm for the phosphors combined with ZnS, ZnO, and ZnSe, respectively. These peaks agree well with the bandgap of ZnS, ZnO, and ZnSe. Moreover, these excitation bands exhibit good continuity, and the excitation spectrum maintains considerable intensity in the entire band. That is, the broadening of the excitation band is closely related to the combination with semiconductors.

The excitation spectra of the samples with different Tb and Yb fractions were recorded [Fig. 3(c)] to investigate the ET processes in the ZnSe/phosphor heterostructure. An increase in Yb fraction causes the spectrum intensity to increase initially and then decrease. It is important to note, however, that with the Yb fraction maintained at 0.06, the Yb^{3+} NIR emission intensity increases by approximately two times when the Tb fraction is increased from 0.005 to 0.010, as shown in the excitation spectra of samples E and C. This result demonstrates that Tb^{3+} acts as a bridge in energy migration from ZnSe to Yb^{3+} ions.

ET process in the Tb^{3+}-Yb^{3+} couple can be verified by studying the lifetime of Tb^{3+} $^5D_4$ level. PL decay was measured by monitoring the 544 nm emission from Tb^{3+} $^5D_4\rightarrow{}^7F_5$ transition for samples A, B, C, and D. The excitation wavelength was 484 nm. Increasing the Yb^{3+} fraction from x = 0 to 0.10 causes the lifetime of Tb^{3+} $^5D_4\rightarrow{}^7F_5$ transition to decrease monotonically from 1.17 ms to 0.56 ms. ET from Tb^{3+} to Yb^{3+} ions is thus well supported.

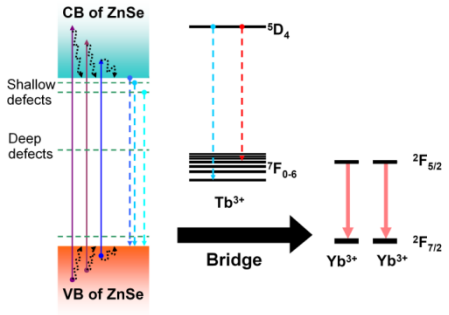

Fig. 4. ET diagrams in the ZnSe/phosphor heterostructure.

Based on these results, we conclude that the broadband down-conversion designed in Fig. 1 has been achieved. Figure 4 shows the ET diagram in ZnSe/phosphor heterostructure. The ZnSe phase absorbs the high-energy photons through band-to-band transition, and then relaxes the photogenerated carriers to its band edge and some defect levels, and finally sensitizes the Yb^{3+} $^2F_{5/2}\rightarrow{}^2F_{7/2}$ emission through the bridge effect of Tb^{3+} $^5D_4\rightarrow{}^7F_6$ transition. In other words, the ET process is primarily composed of the transfer from ZnSe to Tb^{3+} and QC down-conversion in the Tb^{3+}-Yb^{3+} couple. Nevertheless, the possibility of direct ET from ZnSe to Yb^{3+} ions cannot be completely discounted. The excitation band was expanded to 550 nm, covering a part of green light with energy lower than the ZnSe bandgap. This part of excitation originates from the absorption of deep defects in ZnSe.

#201619 - $15.00 USD Received 19 Nov 2013; revised 11 Feb 2014; accepted 20 Feb 2014; published 1 Apr 2014

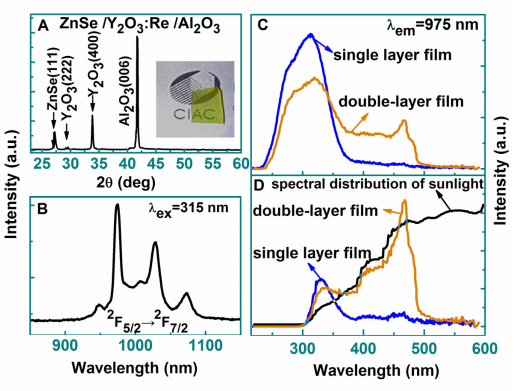

Fig. 5. (A) XRD pattern and photograph of the ZnSe/ Y_2O_3:[(Tb^{3+}-Yb^{3+}), Li^+] double-layer thin films. Inset: a photograph of the double-layer film. (B) NIR PL spectrum of Yb^{3+}, excited at 315 nm. (C) excitation spectra of Yb 975-nm emission of phosphor single-layer thin film and ZnSe/Y_2O_3:[(Tb^{3+}-Yb^{3+}), Li^+] double-layer thin film. (D) The "corrected" excitation spectra of the above samples with considering the sunlight spectral distribution. The spectral distribution of sunlight is also shown here.

The above experiments and analysis demonstrate the ET processes and the feasibility of ZnSe/Y_2O_3:[(Tb^{3+}-Yb^{3+}), Li^+] heterostructure acting as a broadband down converter. However, a practical down-converter should be fabricated into a transparent material. Therefore, another ZnSe/phosphor heterostructure, double-layer film, was fabricated. This film contains a phosphor film on a sapphire substrate and a ZnSe cap layer, which were prepared by magnetron sputtering and physical vapor deposition, respectively. The XRD pattern of the double-layer film is shown in Fig. 5(a). The strong [400] peak of the phosphor at 33.7° and the [111] peak of ZnSe at 27° indicate the preferred orientation of the phosphor and ZnSe layers. A photograph of the double-layer film grown on sapphire is shown as an inset. The sample shows yellow color belonging to ZnSe. Through the sample, the letters "AC" on the paper can be observed clearly, indicating its good transparence. Figure 5(b) shows the Yb^{3+} emission spectrum of the double-layer thin film. Figure 5(c) shows the excitation spectra of Yb^{3+} NIR emission in the single phosphor film and ZnSe/phosphor double-layer film, both of which were measured by monitoring at 975 nm. As expected, the latter exhibits a broad excitation band similar to that of the ZnSe/phosphor heterostructure fabricated by SPS. Considering the spectral distribution of solar energy, the excitation band should be expanded to the visible region because sunlight that reached the ground contains 44% visible light, much larger than the ultraviolet fraction of 3% to 4%. Figure 5(d) shows the excitation spectral comparison in consideration of the sunlight spectral distribution. The "corrected" excitation spectral curves are obtained by multiplying the normalized solar spectrum. The area under the corrected excitation spectrum curve of the double-layer thin film is significantly larger than that of the single-phosphor thin film. If the heterostructure is fabricated to be a long-period multilayer and possesses high optical quality of the ZnSe thin film, the down-conversion efficiency can be further increased.

4. Conclusions

In conclusion, broadband down-conversion to intense Yb^{3+} NIR emission was realized in the ZnSe/Y_2O_3:[(Tb^{3+}-Yb^{3+}), Li^+] heterostructures. The excitation band of Yb^{3+} NIR emission covers a region from 250 nm to 550 nm, which is much wider than that of the single-phased phosphor. It is attributed to the adequate absorption of high energy photons in ZnSe phase and efficient energy transfer to Tb^{3+}-Yb^{3+} couple. It indicates that Phosphor/semiconductor heterostructure is an effective way to realize the broadband down-conversion based on rare earth ions, which can be used to boost the energy efficiency of silicon solar cells.

#201619 - $15.00 USD Received 19 Nov 2013; revised 11 Feb 2014; accepted 20 Feb 2014; published 1 Apr 2014

Acknowledgments

This work is supported by the National Natural Science Foundation of China under Grants Nos. 51002148, 51372244, 21221061 and 21071141, and by the Natural Science Foundation of Jilin province, China, under grant no. 201115126.

#201619 - $15.00 USD Received 19 Nov 2013; revised 11 Feb 2014; accepted 20 Feb 2014; published 1 Apr 2014